

1-1-1990

## High-Resolution Photoelectron Spectrometry Of Selected Ns' And Nd' Autoionization Resonances In Ar, Kr, And Xe

Jian Z. Wu  
*University of Central Florida*

Scott B. Whitfield  
*University of Central Florida*

C. Denise Caldwell  
*University of Central Florida*

Manfred O. Krause

Peter Van der Meulen

Find similar works at: <http://stars.library.ucf.edu/facultybib1990>  
See next page for additional authors  
University of Central Florida Libraries <http://library.ucf.edu>

This Article is brought to you for free and open access by the Faculty Bibliography at STARS. It has been accepted for inclusion in Faculty Bibliography 1990s by an authorized administrator of STARS. For more information, please contact [STARS@ucf.edu](mailto:STARS@ucf.edu).

---

### Recommended Citation

Wu, Jian Z.; Whitfield, Scott B.; Caldwell, C. Denise; Krause, Manfred O.; Van der Meulen, Peter; and Fahlman, Anders, "High-Resolution Photoelectron Spectrometry Of Selected Ns' And Nd' Autoionization Resonances In Ar, Kr, And Xe" (1990). *Faculty Bibliography 1990s*. 187.  
<https://stars.library.ucf.edu/facultybib1990/187>

---

**Authors**

Jian Z. Wu, Scott B. Whitfield, C. Denise Caldwell, Manfred O. Krause, Peter Van der Meulen, and Anders Fahlman

## High-resolution photoelectron spectrometry of selected $ns'$ and $nd'$ autoionization resonances in Ar, Kr, and Xe

Jian Z. Wu, Scott B. Whitfield, and C. Denise Caldwell  
*University of Central Florida, Orlando, Florida 32816*

Manfred O. Krause and Peter van der Meulen\*  
*Oak Ridge National Laboratory, Oak Ridge, Tennessee 37831*

Anders Fahlman  
*Linköping Institute of Technology, S-58183, Linköping, Sweden*  
 (Received 22 January 1990)

Photoionization cross sections ( $\sigma$ ) and photoelectron angular distribution parameters ( $\beta$ ) across the ( $ns'$ ,  $nd'$ ) autoionization resonances for Ar, Kr, and Xe have been measured with photon resolution widths as low as 0.023 Å by means of synchrotron-based photoelectron spectroscopy. The experimental results are compared with those obtained by other experimental techniques and theoretical results. The enhanced resolution allows a redetermination of the width of the  $ns'$  resonances.

### I. INTRODUCTION

The study of autoionizing resonances of the rare gases in the vacuum ultraviolet region was initiated by Beutler<sup>1</sup> and first theoretically analyzed by Fano.<sup>2</sup> Since then, new and more sophisticated experimental<sup>3-6</sup> and theoretical<sup>7,8</sup> techniques have been developed for studying the dynamics of the ionization process. Electron spectrometry in combination with synchrotron radiation has proven a powerful vehicle to probe many-electron effects in bound and in continuum states, interactions between continuum and bound states, and relativistic effects. Recent theoretical treatments of autoionizing resonances based on multichannel quantum-defect theory<sup>9-13</sup> (MQDT) in conjunction with the relativistic random-phase approximation (RRPA) have yielded all the autoionization parameters for the rare gases.<sup>13</sup> The experimental measurements of key photoionization parameters in the vicinity of these resonances provide sensitive tests for the development of MQDT.

The ionization of an outer  $p$  electron from one of the rare gases yields ions in the ground state,  $^2P_{3/2}$ , and the excited state,  $^2P_{1/2}$ . Rydberg series have been observed converging on the ground state  $^2P_{3/2}$  and on the excited state  $^2P_{1/2}$ . Higher members of the series converging upon  $^2P_{1/2}$  lie in the continuum above the  $^2P_{3/2}$  ionization threshold and are therefore subject to autoionization. The autoionization spectrum consists of two series which arise from transitions from the  $^1S_0$  ground state to excited levels designated as  $(^2P_{1/2})ns'$  or  $(^2P_{1/2})nd'$ , i.e., the excitation of an outer  $p$  electron to  $ns$  or  $nd$  states (in  $J$ - $j$  notation).

Since Beutler's original work, energies and absolute photoionization cross sections of the  $ns'$  and  $nd'$  resonances for Ar, Kr, and Xe have been determined experimentally by a number of workers<sup>14-24</sup> either by photoabsorption or by photoionization. The first measurement of

the variation of the angular distribution parameter  $\beta$  of the Beutler-Fano autoionizing resonances in Xe was made by Samson and Gardner.<sup>25</sup> Later, studies of  $\beta$  were made for Kr and Xe by Morioka *et al.*,<sup>26</sup> and for Xe by Carlson *et al.*<sup>6</sup> Heinzmann *et al.*<sup>27</sup> extended the study of the resonances to the measurement of the spin polarization parameters for photoelectrons of Xe in this same photon energy region. Resolutions in these experiments ranged from 0.4 Å for Morioka *et al.*<sup>26</sup> to 1.2 Å for Carlson *et al.*<sup>6</sup> Thus far, no  $\beta$  measurements have been made at a resolution which approaches the 0.07-Å resolution used for the cross-section determinations.<sup>5</sup> However, concurrently to the present study, a high-resolution measurement of  $\beta$  over the narrow range of the  $8s'$  resonance of Xe was carried out by Tonkyn and White<sup>28</sup> in a laser excitation experiment. For Ar no experiment exists of the variation of the photoelectron angular distribution with energy across the autoionization resonance to complement the cross-section measurement, which was performed at a resolution of 0.02 Å.<sup>17</sup>

In the present paper we report the high-resolution measurements of  $\beta$  and  $\sigma$  across selected autoionizing resonances for Ar, Kr, and Xe. We focus attention on the  $6d'$  and the  $8s'$  levels for Kr and Xe; the  $10d'$  and the  $12s'$  levels for Ar. The resolution we achieved marks the first time that synchrotron-based photoelectron spectrometry measurements have been possible at resolutions comparable to that used in the less demanding photoion and photoabsorption techniques. The enhanced resolution also allows a redetermination of the widths of the  $ns'$  resonances. While the early experimental  $\beta$  values of Samson and Gardner<sup>25</sup> have been compared with theoretical MQDT values by Dill<sup>29</sup> and by Geiger,<sup>12</sup> our experimental values of  $\beta$  and  $\sigma$  for Ar, Kr, and Xe are compared with recent MQDT calculations by Johnson *et al.*<sup>13</sup> and available high-resolution measurements by others.<sup>4,15,16,28</sup>

## II. EXPERIMENT

The photoelectron spectrometry studies were carried out at the 4-m Normal Incidence Monochromator (NIM) at the University of Wisconsin Synchrotron Radiation Center. The apparatus we use for all measurements has been described in detail elsewhere.<sup>30,31</sup> It will suffice to give a limited description of those features appropriate to our experiments. Radiation from the 4-m NIM falls onto a source of Ar, Kr, or Xe. Electrons ejected from the atoms are energy analyzed in an electrostatic analyzer having 1% energy resolution and monitored with a channeltron detector. Three analyzers mounted on a platform that can be rotated in a plane perpendicular to the direction of incidence of incoming radiation allow ready determination of both  $\beta$  and  $\sigma$ .

In the dipole approximation the angular distribution of intensity of photoelectrons is given by

$$I(\theta) \propto \frac{d\sigma}{d\Omega} = \frac{\sigma}{4\pi} \left[ 1 + \frac{\beta}{4} [1 + 3p \cos(2\theta)] \right] \quad (1)$$

where  $p$  is the photon polarization and  $\theta$  is the angle relative to the major electric vector of the polarized photon beam.  $\beta$  is the electron angular distribution parameter, and  $\sigma$  is the photoelectron cross section. The differential cross section  $d\sigma/d\Omega$  is proportional to the observed intensity,  $I(\theta)$ , and by measuring  $I(\theta)$  at  $\theta=0^\circ$  (or  $180^\circ$ ) and  $\theta=90^\circ$ , the  $\beta$  parameter is obtained from

$$\beta = \frac{4(R-1)}{3p(R+1)-(R-1)} \quad (2)$$

where  $R = I(0^\circ)/I(90^\circ)$  or  $I(180^\circ)/I(90^\circ)$ .

Since the intensity measurements were taken simultaneously with two analyzers set at right angles, any effects on  $\beta$  from fluctuations and drifts in source gas pressure and photon flux could be eliminated. For a given  $p$ , cross-section measurements are taken at the so-called magic angle  $\theta_m = \frac{1}{2} \cos^{-1}[1/(3p)]$ , at which the  $\beta$ -dependent term should make no contribution to the intensity. We also calculated  $\sigma$  from the data obtained simultaneously at  $\theta=0^\circ$  and  $\theta=90^\circ$  as a supplement to the direct determination at  $\theta_m$ . Possible deviations of the electron source from a homogeneous cylinder with regard to the viewing angle were checked by recording photoelectrons having an isotropic angular distribution. We use for this purpose the Ar  $3p$  photoelectron at  $h\nu=16.5$  eV, for which  $\beta=0.00 \pm 0.06$ .<sup>3</sup> The required corrections amounted to about 10% in the ratio  $R$ . The relative response of the analyzers was determined by measuring the signal strengths for each analyzer at the same angle  $\theta$ , e.g.,  $\theta=45^\circ$ .

The polarization of the photon beam was obtained from a measurement of the angular distributions [Eq. (2)] of Ar  $3p$ , Kr  $4p$ , and Xe  $5p$  at 21.22 eV, for which  $\beta$  values are known to an accuracy better than  $\pm 0.04$ . We found a value of  $p=0.77(3)$ . Tests at lower photon energies proved the polarization to have the same value within the error limit.

Two different modes were employed for data recording: the constant ionic state (CIS) mode, in which spectra

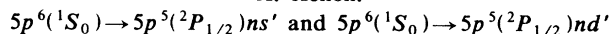
are recorded by scanning simultaneously the photon energy and accelerating voltage of the source cell so as to always observe electrons corresponding to the same final ionic state; and the photoelectron spectroscopy (PES) mode, in which spectra are taken at constant photon energy by scanning the photoelectron energy. CIS spectra are normalized with the aid of PES spectra. Signals were stored in a multichannel scalar which could be multiplexed. The step width for the CIS scan was typically 0.2 meV.

The resolution for a CIS scan depends solely on the bandpass of the monochromator. Our intensity levels were such that we could typically work with slit settings as narrow as  $25 \mu\text{m}$ . For the 3600-line/mm Au grating used, this led to a bandpass of  $0.023(1) \text{ \AA}$ . However, such a narrow bandpass was only necessary for the measurements on Ar. The widths of the lines are such that we could work with slit openings of  $30 \mu\text{m}$  for Kr and Xe, and even  $75 \mu\text{m}$  for Xe without loss of information. The corresponding bandpass for these widths was  $0.026(2)$  and  $0.05(1) \text{ \AA}$ , respectively, as determined by measurements on the Xe  $ns'$  series,  $n=8-14$ , and on the Ne ( $13d'$ ,  $14s'$ ) and ( $14d'$ ,  $15s'$ ) resonances.<sup>32</sup>

The gas pressure in the source volume was approximately  $2 \times 10^{-4}$  Torr. With a pressure of less than  $3 \times 10^{-6}$  Torr in the analyzer region, scattering processes of the electrons at  $30 < E_{\text{kin}} < 800$  meV in the source and  $E'_{\text{kin}} = 5$  eV upon entering the analyzers could be neglected. All data were corrected for variations in photon flux, analyzer response, background counts, and asymmetry of the source volume. In the case of CIS spectra, photoelectron spectra were taken at suitable photon energies near the beginning and the end of the CIS scan to provide the needed information for the corrections. In addition, the signal from a Ni mesh located at the exit mirror of the NIM served for normalization.

## III. EXPERIMENTAL RESULTS AND DISCUSSION

### A. Xenon:



The experimental results for  $\beta$  and  $\sigma$  as a function of photon energy are shown in Fig. 1. The solid lines are CIS spectra; the points with errors bars represent the values of PES measurements used for normalization. Because of the repetition of  $\sigma$  and  $\beta$  along the Rydberg series, we shall focus on the first autoionizing resonance between the  $^2P_{3/2}$  and  $^2P_{1/2}$  ionization thresholds, i.e., the  $n=8$  line in the  $s'$  series and the  $n=6$  line in the  $d'$  series. In Fig. 1 the variation of  $\beta$  is compared with the variation of  $\sigma$  in passing through the autoionizing resonances ( $6d'$ ,  $8s'$ ). One notes the characteristic pattern in  $\sigma$ : a narrow "s" structure superimposed on a broad "d" structure and a large peak-to-peak ratio of the  $s$  to  $d$  resonance, as reported earlier in a number of papers.<sup>5,17</sup> The energy scale of  $\sigma$  in Fig. 1 is normalized at the  $8s'$  peak to 12.5753 eV, according to Moore's tables.<sup>21</sup> The  $\sigma$  spectrum was converted to an absolute cross section by normalization to the theoretical calculation by Johnson *et al.*<sup>13</sup> at 12.650 eV.

In Fig. 2 results of theoretical calculations for both  $\sigma$  and  $\beta$  by Johnson *et al.*<sup>13</sup> and earlier experimental data for  $\sigma$  obtained in photoion measurements by Eland<sup>5</sup> and for  $\beta$  in photoelectron measurements by Samson and Gardner<sup>25</sup> are reproduced for comparison with our experimental results. All curves are adjusted to have equal energy at the  $8s'$  resonance. The  $\sigma$  data of Eland<sup>5</sup> are also normalized at 12.650 eV to the theoretical result of Johnson *et al.*<sup>13</sup> In the determination of  $\sigma$  the results of the ion measurement and the photoelectron measurement essentially overlap except at the maximum of the  $8s'$  resonance. Determination of cross sections in regions through which  $\beta$  is rapidly varying requires that the possible influence of  $\beta$  is removed by a careful alignment of the electron detector at the "magic angle"  $\theta_m$ . In our case,  $p=0.77$  and  $\theta_m=57.8^\circ$ . However, this number can vary by as much as  $3^\circ$  within the 0.03 error limit of the measurement of  $p$ . The orientation of the electric field vector is determined at the same time as the asymmetry in the source volume and is known to within  $\pm 5^\circ$ . Taking

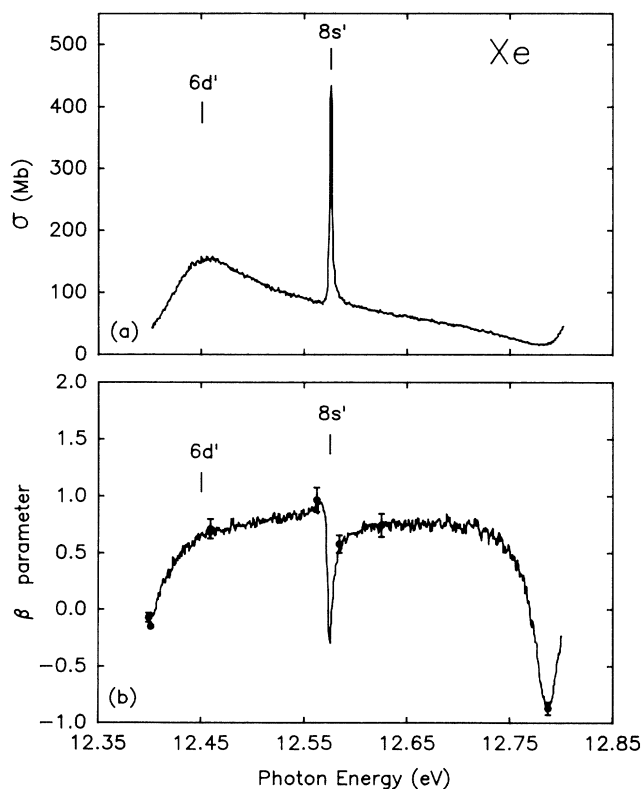


FIG. 1. The cross section  $\sigma$  (a) and angular distribution parameter  $\beta$  (b) of xenon photoelectrons across the ( $6d'$ ,  $8s'$ ) autoionization resonances. The solid lines are the CIS data; PES results are indicated by points with error bars. The energy scale is fixed at  $E(8s')=12.5753$  eV. The  $\sigma$  curve is normalized at 12.650 eV to 61.1 Mb according to Ref. 13. The CIS spectrum for  $\sigma$  was taken with 0.5 meV/step at a resolution of  $0.026 \text{ \AA}$  [ $\Delta E=0.33\pm 0.03$  meV]; the CIS spectrum for  $\beta$  was taken with 0.2 meV/step at a resolution of  $0.05 \text{ \AA}$  [ $\Delta E=(0.69\pm 0.03)$  meV]. Each spectrum contains 801 points.

both sources of error into account, we estimate that the setting of the electron analyzer at the magic angle could have a maximum uncertainty of  $8^\circ$ . As  $\beta$  is so large at the  $8s'$  resonance, this could give rise to an error on the order of 12% in the maximum of the  $8s'$  resonance. Within this limit, the ion result and the photoelectron result for the peak value are in accord.

The  $\beta$  spectrum across the  $8s'$  resonance varies from  $\beta=1.0$  to  $\beta=-0.3$ . This is a sharper variation than observed previously in the experiments done at lower resolution.<sup>6,25,26</sup> Our results, which have an accuracy of  $\pm 0.07$  in  $\beta$  show that the minimum in  $\beta$  for the  $8s'$  resonance is a much sharper spectral feature than was predicted by theoretical calculations of Dill<sup>29</sup> and Johnson *et al.*<sup>13</sup> In particular, the  $\beta$  value around the  $8s'$  resonance has a more pronounced dip ( $\beta=-0.3$ ) in the experiment than in the calculation ( $\beta=0$ ).<sup>13</sup> The sharper dip in  $\beta$  is accompanied by a narrower observed width of the  $8s'$  peak than predicted by theory. Also, near the maximum of the  $6d'$  resonance there is a discrepancy in both  $\beta$  and  $\sigma$  between theory and experiment, with the experiment displaying a sharper onset.

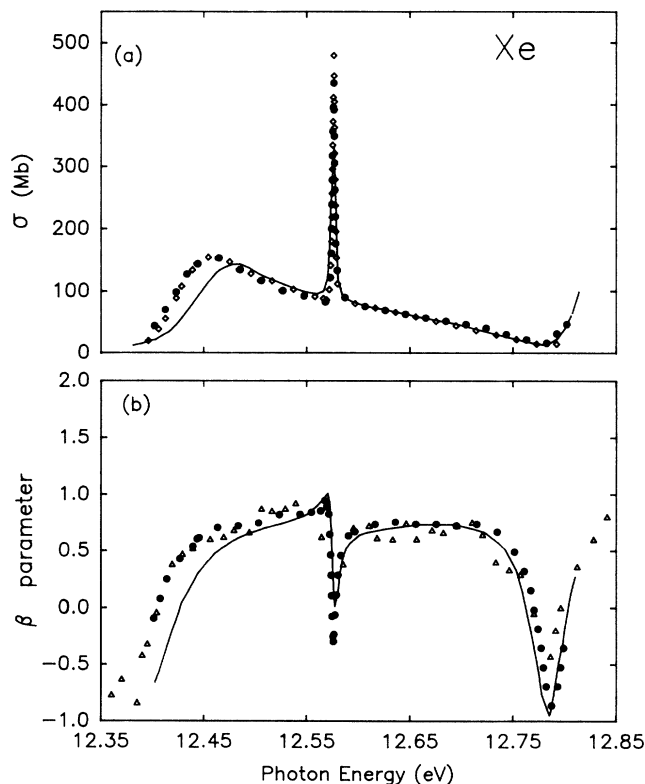


FIG. 2. Angular distribution parameter  $\beta$  and cross section  $\sigma$  for Xe across the ( $6d'$ ,  $8s'$ ) autoionization resonances. Solid circles are this work; open triangles are experimental data by Samson and Gardner (Ref. 25); open diamonds are experimental data by Eland (Ref. 5); solid lines (both panels) are the theoretical MQDT-RRPA results of Johnson *et al.* (Ref. 13). All curves are set equal in energy at the  $8s'$  resonance, and the cross sections are normalized to the theoretical results at 12.650 eV.

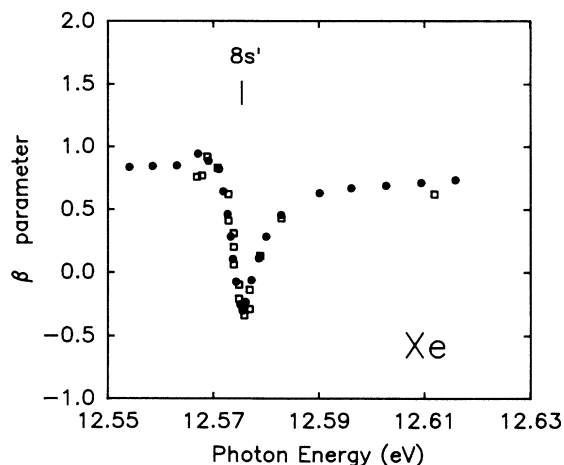
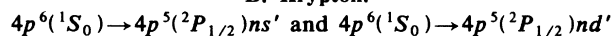


FIG. 3. Angular distribution parameter  $\beta$  for Xe across the  $8s'$  resonance. Solid circles are this work, obtained with a resolution of  $0.026 \text{ \AA}$  [ $\Delta E = (0.33 \pm 0.03) \text{ meV}$ ]. Open squares are the experimental data of Tonkyn and White (Ref. 28), obtained with a resolution of  $0.02 \text{ \AA}$  ( $\Delta E = 0.26 \text{ meV}$ ) using laser excitation.

The recent experiment by Tonkyn and White<sup>28</sup> using laser excitation reveals the same sharp structure of  $\beta$  near the  $8s'$  resonance. As can be seen in Fig. 3, our values of  $\beta$  for the  $8s'$  resonance overlap exactly with those obtained by Tonkyn and White. This accord, which applies also to the absolute values of  $\beta$ , is remarkable and gratifying in view of the different techniques applied in the two experiments. Since the natural width of the resonance is evidently much larger than the instrumental resolution of  $0.33 \text{ meV}$  in our experiment and  $0.26 \text{ meV}$  in the laser experiment,<sup>28</sup> the observed width is essentially the same in both experiments. To an excellent approximation, we are scanning the Xe ( $6d'$ ,  $8s'$ ) resonances—and, as seen in the following, also the Kr ( $6d'$ ,  $8s'$ ) resonances—with negligible instrumental broadening.

#### B. Krypton:



In Fig. 4 we show  $\sigma$  and  $\beta$  results obtained in the region of the ( $6d'$ ,  $8s'$ ) resonances for Kr. The upper panel gives the autoionization cross sections; the lower panel gives the corresponding  $\beta$  values. The  $\sigma$  curve is converted to an absolute cross section by normalization to the theoretical value<sup>13</sup> of  $\sigma = 37.1 \text{ Mb}$  at  $14.155 \text{ eV}$ .

The  $\beta$  curve we report here is the first measurement of  $\beta$  for this resonance structure in krypton. As was the case for Xe, there is a deep dip in the vicinity of the  $8s'$  feature, with  $\beta = -0.64$  at  $14.101 \text{ eV}$ . The variation in  $\beta$  ( $0.51$  to  $-0.61$ ) across the resonance is  $\Delta\beta = 1.15$ . The entire  $\beta$  curve is shifted downward, on the average by  $0.4$ , compared with the  $\beta$  curve of Xe. In addition, the  $8s'$  and the maximum of the  $6d'$  level are more closely spaced for Kr than for Xe. The uncertainty in the  $\beta$  values is about  $0.07$ .

Figure 5 shows the comparison between our measurements of  $\beta$  and  $\sigma$  for Kr near the ( $6d'$ ,  $8s'$ ) resonances

and the theoretical predictions by Johnson *et al.*<sup>13</sup> Also, the  $\sigma$  data of the earlier ion current measurement,<sup>5</sup> normalized at  $14.155 \text{ eV}$  to the value of Johnson *et al.*,<sup>13</sup> are reproduced in the figure. All curves are set equal in energy at the  $8s'$  resonance for the purpose of comparison. As was the case with Xe, both experimental results agree quite well except at the maximum of the  $8s'$  resonance. Even though there is a possible 12% error associated with the photoelectron measurements due to the influence of  $\beta$  on intensity at the magic angle, the value of the peak is still less than that from the photoion measurement. Our experimental results are an average of three independent determinations, one from  $\sigma$  at the magic angle and the other two from the results of intensity measurements at  $0^\circ$  and  $90^\circ$  for  $\beta$ . These agree to within 13% of each other. As the experimental widths of both the photoion results and the photoelectron results are comparable, the difference cannot be explained on the basis of resolution. In addition, the natural width of this line is  $1.43 \text{ meV}$ , so any resolution better than  $0.05 \text{ \AA}$  should not influence the observed width. With all sources of error taken into account, our result remains 20% lower than the photoion measurement at the maximum of the  $8s'$  peak, and the origin of this discrepancy is unclear.

The general agreement in the structure and in the behavior of  $\beta$  and  $\sigma$  between theory and experiment is

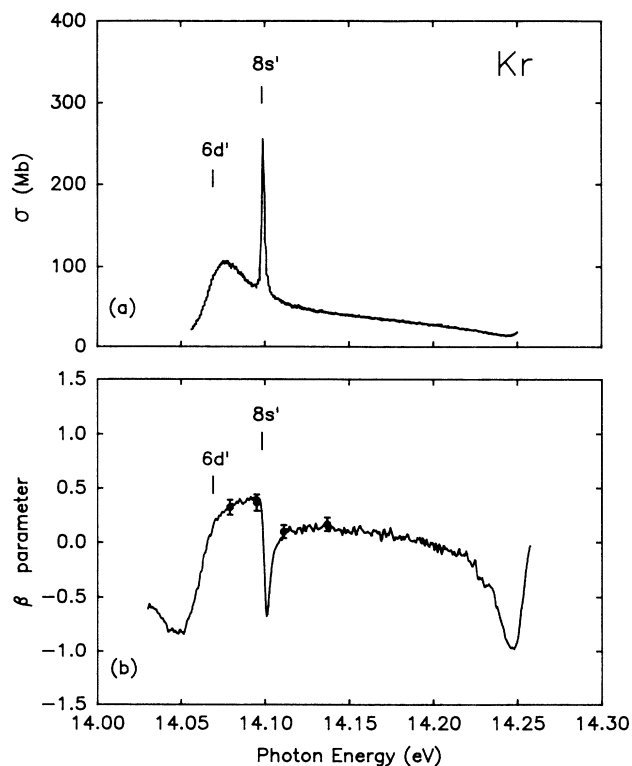


FIG. 4. Cross section  $\sigma$  (a) and angular distribution parameter  $\beta$  (b) of Kr photoelectrons in the region of the ( $6d'$ ,  $8s'$ ) resonances. Solid lines are the CIS spectra, obtained at  $\Delta\lambda = 0.026 \text{ \AA}$ ,  $\Delta E = (0.40 \pm 0.03) \text{ meV}$ , with a mesh size of  $0.2 \text{ meV}$ . The points with error bars are the PES results.

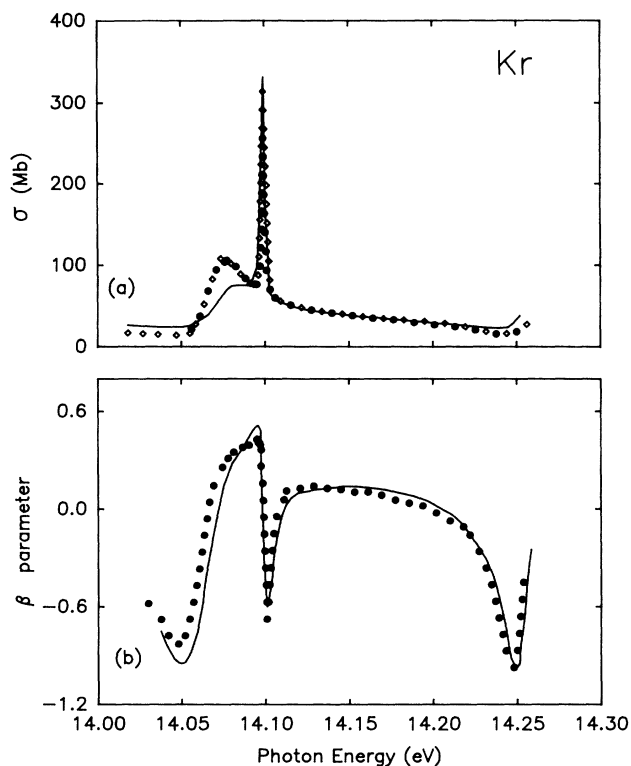


FIG. 5. Angular distribution parameter  $\beta$  and photoionization cross section  $\sigma$  for Kr across the ( $6d'$ ,  $8s'$ ) resonances. Solid circles (both panels) are this work. (Only every 40th point is shown.) Open diamonds (upper panel) are taken from Berkowitz (Ref. 5); solid lines (both panels) are MQDT-RRPA calculations by Johnson *et al.* (Ref. 13). All curves are set equal in energy at the  $8s'$  resonance. The experimental cross-section results are normalized to the theoretical value at 14.155 eV.

good. We notice, however, discrepancies, albeit smaller ones, of the same type as those for Xe. The observed width of the  $8s'$  resonance is slightly narrower than the calculated width, and the  $6d'$  resonance is somewhat wider, with a sharper onset than predicted by theory.

### C. Argon:

$$3p^6(^1S_0) \rightarrow 3p^5(^2P_{1/2})12s' \text{ and } 3p^6(^1S_0) \rightarrow 3p^5(^2P_{1/2})10d'$$

The results of  $\sigma$  and  $\beta$  measurements for the ( $10d'$ ,  $12s'$ ) resonances in Ar are shown in Fig. 6. We selected the second pair of ( $nd'$ ,  $ns'$ ) series above the  $^2P_{3/2}$  threshold instead of the first, as in Kr and Xe, in order to avoid the region of very low electron kinetic energy. An auxiliary measurement of  $\sigma$  by us using an ion detector is in excellent agreement with the photoelectron recording. Comparison of the data with theoretical calculations by Johnson *et al.*<sup>13</sup> and with earlier photoion measurements reported by Radler and Berkowitz<sup>17</sup> is made in Fig. 7. As seen in the figure, there is good agreement between the two sets of experimental data. Both show clearly that the experimental width observed for the  $12s'$  resonance is determined by the photon bandpass. This is in contrast to the observation in Kr and Xe,

where the width of the  $8s'$  resonance was dominated by the natural width. By fitting the experimental data to a Fano profile, including the effect of the bandpass, we estimate the natural width of the Ar  $12s'$  resonance to be  $0.24(2)$  meV.

The resonance features observed in Ar retain the typical structure which appears in Kr and Xe. However, from Fig. 6, we see that the  $12s'$  peak and the maximum of the  $10d'$  resonance lie closer in energy for Ar than for Kr and Xe. The two peaks in Ar are barely resolved even at a resolution of  $0.02 \text{ \AA}$ .<sup>17</sup> Through the Ar resonances the  $\beta$  parameter continues its trend toward lower values when going from Xe to Kr to Ar. However, for Ar the theoretical  $\beta$  shows a much larger variation than the experimental values in the region of the  $12s'$  resonance. This is primarily, if not entirely, an effect of the limited resolution of the experiment. In analogy with Kr and Xe, we expect the theoretical prediction to be a quite good representation of the  $\beta$  variation around the  $12s'$  feature. However, the depth of the broad minimum occurring on the low-energy side of the  $10d'$  resonance is overestimated by theory. For this feature the experiment is not resolution limited.

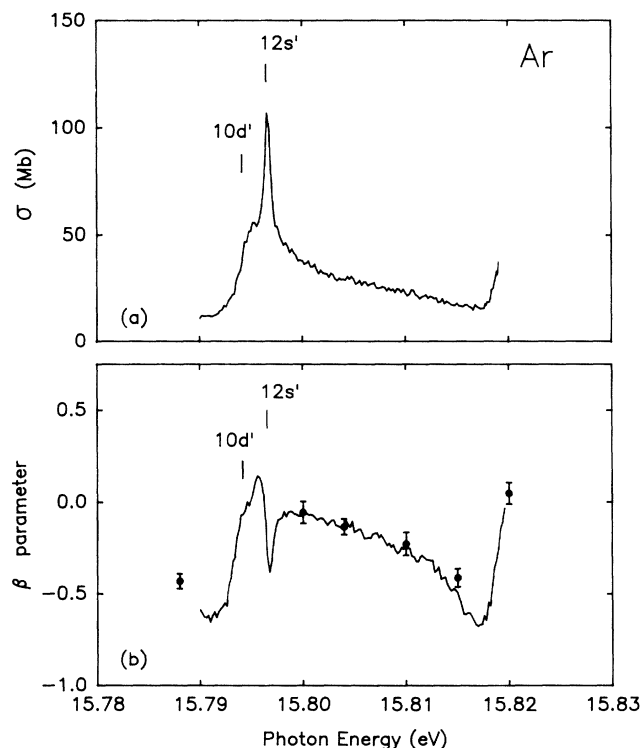


FIG. 6. Cross section  $\sigma$  (a) and angular distribution parameter  $\beta$  (b) of Ar photoelectrons across the ( $10d'$ ,  $12s'$ ) autoionization resonances. Solid lines are the CIS data, obtained at a resolution of  $\Delta\lambda=0.023 \text{ \AA}$ , corresponding to  $\Delta E=(0.46\pm 0.02)$  meV, with a mesh size of  $0.1 \text{ meV}$ . The points with error bars are the PES results. The  $\sigma$  curve is normalized to  $27.5 \text{ Mb}$  at  $15.806 \text{ eV}$ , according to Ref. 13.

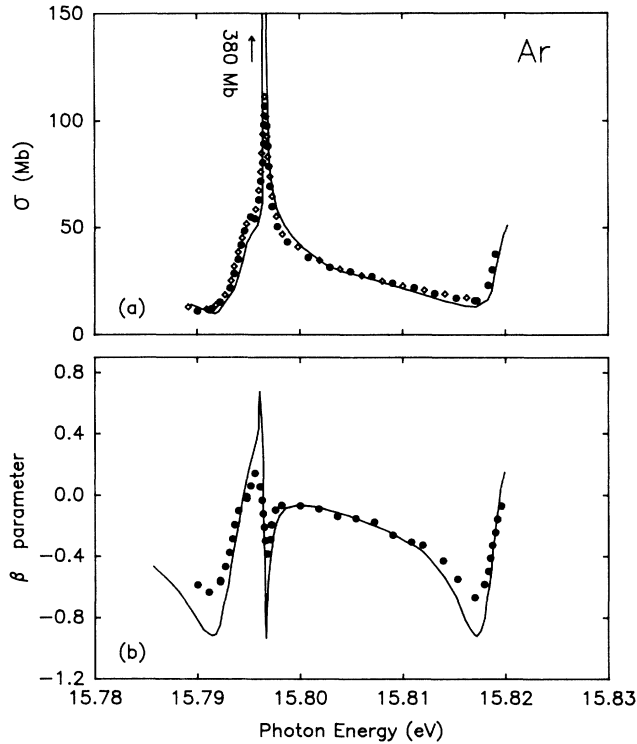


FIG. 7. Cross section  $\sigma$  and angular distribution parameter  $\beta$  for Ar across the ( $10d'$ ,  $12s'$ ) autoionization resonances. Solid circles (both panels) are this work; open diamonds (a) are photoion results reported by Radler and Berkowitz (Ref. 17). Solid lines (both panels) are the MQDT-RRPA results of Johnson *et al.* (Ref. 13). All curves are set equal in energy at the  $12s'$  resonance, and both experimental  $\sigma$  curves are normalized to the theoretical value at 15.806 eV.

#### IV. FANO PARAMETRIZATION OF AUTOIONIZATION RESONANCES

The profile of an isolated autoionizing resonance can be described through the parametric form developed by Fano:<sup>2</sup>

$$\sigma = \sigma_a \frac{(\epsilon + q)^2}{1 + \epsilon^2} + \sigma_b. \quad (3)$$

Here

$$\epsilon = (\omega - \omega_R) / (\Gamma/2) \quad (4)$$

describes the departure of the incident photon energy  $\omega$  from the resonance energy  $\omega_R$  scaled by  $\Gamma/2$ , where  $\Gamma$  is the resonance width. The quantity  $q$  is called the profile index. The quantities  $\sigma_a$  and  $\sigma_b$  represent values for two portions of the cross section describing transitions to states in the continuum that do and do not interact with the discrete autoionizing state, respectively. By least-squares fitting Eqs. (3) and (4) to the experimental data, these five parameters,  $\sigma_a$ ,  $\sigma_b$ ,  $\omega_R$ ,  $\Gamma$ , and  $q$ , can be determined. Alternative parametrizations and fitting procedures have been discussed by Shore<sup>33</sup> and Ueda.<sup>24,34</sup>

To obtain the natural linewidth  $\Gamma$ , one must deconvolute the experimental line shape with a function that is representative of the influence of the width of the exciting radiation and the level of origin of the electron. In our case, this function is well represented by the Lorentzian distribution

$$L(x) = \frac{(B/2\pi)}{x^2 + (B/2)^2} \quad (5)$$

where  $B$  is the full width at half maximum (FWHM) width (bandpass) for this function. In our case there is no contribution from the level of origin of the electron, as we excite from the ground state. The experimental broadening is determined solely by the bandpass of the monochromator, which is equal to 0.023 Å in the case of Ar and 0.026 Å for Kr and Xe. The observed spectrum  $O(\omega)$  is the convolution of the true spectrum [Eq. (3)] and the function (5):

$$O(\omega) = \int_{-\infty}^{\infty} \sigma(\omega - x) L(x) dx. \quad (6)$$

The integral (6) can be evaluated by using contour integration, which leads to

$$O(\omega) = \sigma'_a \frac{(\epsilon' + q)^2}{1 + \epsilon'^2} + \sigma'_b \quad (7)$$

TABLE I. Line-shape parameters obtained through the fitting procedure from the photoionization cross sections of Ar, Kr, and Xe across selected ( $nd'$ ,  $ns'$ ) resonances measured in this work. In the table,  $\omega_R$  is the resonance energy (eV),  $\Gamma$  is the resonance width (meV),  $q$  is the profile index,  $\sigma_a$  is a portion of the cross section describing the transition to states in the continuum that interact with the discrete autoionizing state, and  $\sigma'_b$  is the nonresonant portion of the cross section.  $\sigma_a$  and  $\sigma'_b$  are in units of Mb. The absolute energy scale is derived by setting the value of the energy at the  $8s'$  peak for Kr and Xe and the  $12s'$  peak for Ar to the Moore result (Ref. 21).

		12s'	10d'
Ar	$\omega_R$	15.7974(4)	15.7941(6)
	$\Gamma$	0.24(2)	4.08(1)
	$q$	8.29(3)	1.44(8)
	$\sigma_a$	6.03(3)	50.00(5)
	$\sigma'_b$		14.29(1)
		8s'	6d'
Kr	$\omega_R$	14.0984(4)	14.0692(6)
	$\Gamma$	1.43(3)	25.54(5)
	$q$	82.56(4)	1.99(4)
	$\sigma_a$	0.0356(5)	23.94(5)
	$\sigma'_b$		11.13(1)
		8s'	6d'
Xe	$\omega_R$	12.5750(4)	12.4269(6)
	$\Gamma$	2.33(3)	80.78(8)
	$q$	12.35(4)	1.41(8)
	$\sigma_a$	1.91(3)	34.97(7)
	$\sigma'_b$		2.03(1)



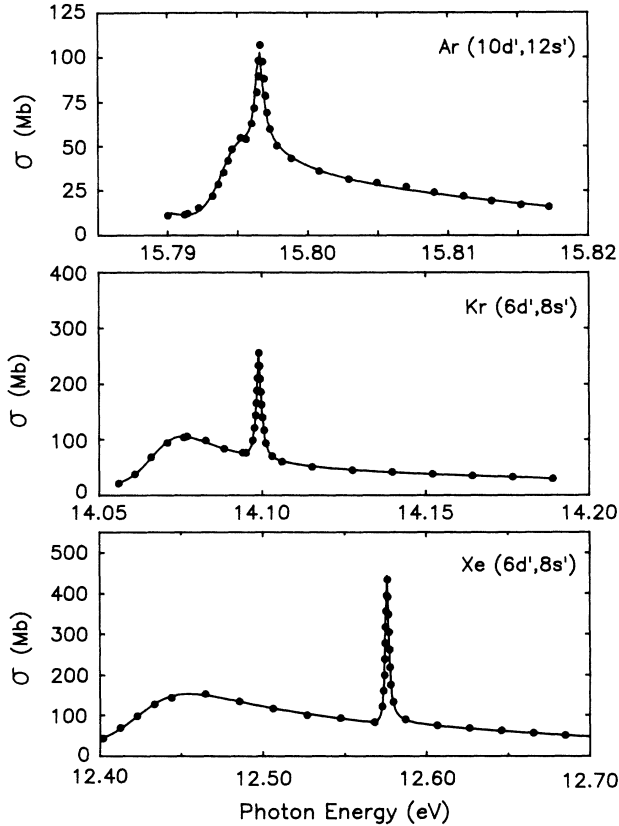


FIG. 8. Photoionization cross section  $\sigma$  across selected ( $nd'$ ,  $ns'$ ) resonances for Ar, Kr, and Xe. Solid circles are this experiment; solid lines are fitted curves using Eqs. (12) and (13), together with Eqs. (8)–(11). Parameters of the best fits for these resonances are listed in Table I. For the sake of clarity, only every 40th point is shown outside the  $s'$  resonances.

where

$$\epsilon' = (\omega - \omega_R) / (\Gamma' / 2), \quad (8)$$

$$\Gamma' = \Gamma + B, \quad (9)$$

$$\sigma'_a = \frac{\sigma_a}{1 + (B/\Gamma)}, \quad (10)$$

and

$$\sigma'_b = \sigma_b + (B/\Gamma)\sigma'_a. \quad (11)$$

Equation (7) has the same parametric form as the original Fano expression. There are six parameters,  $\sigma_a$ ,  $\sigma_b$ ,  $\omega_R$ ,  $\Gamma$ ,  $q$ , and  $B$ , to be employed in fitting Eqs. (7)–(11) to a single line of the Ar, Kr, or Xe spectrum. However, in the absence of the  $s$ - $d$  interactions, which we assume heuristically to be the case here, it is possible to fit the two lines to a superposition of two functions of the form (7):

$$O(\omega) = \sigma'_{as} \frac{(\epsilon'_s + q_s)^2}{1 + \epsilon_s'^2} + \sigma'_{ad} \frac{(\epsilon'_d + q_d)^2}{1 + \epsilon_d'^2} + \sigma'_b \quad (12)$$

where

$$\epsilon'_i = (\omega - \omega_{Ri}) / (\Gamma'_i / 2) \text{ for } i = s \text{ and } d. \quad (13)$$

The detailed description of the fitting of two or more lines was given by Ueda.<sup>24,34</sup>

The parameters from the best fits to the data are given in Table I; comparisons of the fitted curves and the experimental results are given in Fig. 8. The errors associated with  $\Gamma_n$  are determined largely from the uncertainty in the bandpass. Other errors are those derived from the accuracy of the fit.

In order to better establish the widths of the lines, higher levels of the  $ns'$  Rydberg series for Kr and Xe were also measured in this experiment. Fano parameters from a best fit of these lines are given in Table II. In the fourth column of this table are given the widths for Kr and Xe calculated according to the relationship  $\Gamma_c \propto 1/(n - \delta)^3$ , where  $\delta$  is taken from the resonance energies quoted in the second column. For Kr,  $\delta = 3.1014$  and for Xe,  $\delta = 4.0053$ . As can be seen, the agreement between the two determinations is excellent.

TABLE II. Widths of the  $ns'$  resonances of Ar, Kr, and Xe.  $\Gamma_n$  is obtained through fitting via the Fano parametrization, Eqs. (7)–(11).  $\Gamma_c$  is calculated from  $\Gamma_c \propto 1/(n - \delta)^3$ , where  $\delta$  is obtained from the resonance energies given in the second column.  $\Gamma_a$  is taken from Ref. 16. The resonance energies,  $\omega_0$ , are calculated from the Moore table (Ref. 21) [with  $\omega_0(\text{eV}) = \omega_0(\text{cm}^{-1})(12\,398.52)10^{-8}$ ].

Features $ns'$	Resonance energy (eV)		Autoionization width (meV)		
	$\omega_0$	$\Gamma_n$	$\Gamma_c$	$\Gamma_a$	
Ar 12	15.7974	0.24(2)		0.298	
Kr 8	14.0985	1.43(3)	1.43	1.42	
	14.2742	0.86(3)	0.82	0.929	
	14.3774	0.46(3)	0.51		
	14.4944	0.24(3)	0.24		
Xe 8	12.5753	2.33(3)	2.24	1.83	
	12.8888	1.05(3)	1.14	1.09	
	13.0576	0.60(3)	0.66		
	13.2240	0.33(3)	0.28		
	13.3009	0.18(3)	0.14		

## V. CONCLUSION

Working for the first time in a photoelectron spectrometry experiment at a resolution comparable to photoabsorption and photoion techniques, we have completed a study of selected  $ns'$  and  $nd'$  resonance features in Ar, Kr, and Xe. For the first time, both the cross section  $\sigma$  and the angular distribution parameter  $\beta$  were measured for these gases, allowing us to reevaluate the most advanced theoretical model, the RRPA MQDT, in a rather comprehensive way. We find general good accord in all cases. However, we note a number of small, but significant discrepancies. In particular, the width of the  $8s'$  autoionization resonances of Kr and, especially, Xe is overestimated by theory. It appears that the strengths of interaction of the strongly interacting channels considered in the calculation should be reexamined.

The cross sections are parametrized with the aid of the Fano resonance line-shape formula. The data reveal the

structure of  $\sigma$  and  $\beta$  in the vicinity of the first  $ns'$  and  $nd'$  resonances of Kr and Xe without instrumental broadening. The same applies to the  $10d'$  resonance of Ar, but the  $12s'$  resonance of Ar is too narrow to be studied equally well at the present level of photon energy resolution available.

## ACKNOWLEDGMENTS

This work was supported in part by the National Science Foundation (NSF) under Grant Nos. PHY-8701193 and PHY-8707550, and by U.S. Department of Energy, Division of Chemical Sciences, Office of Basic Energy Research, under Contract No. DE-AC05-85OR21400 with Martin Marietta Energy Systems, Inc. The University of Wisconsin Synchrotron Radiation Center is operated under NSF Grant No. DMR-8821625. Peter van der Meulen acknowledges partial support by the Netherlands Organization for Scientific Research.

\*On leave from University of Amsterdam, The Netherlands.

<sup>1</sup>H. Beutler, *Z. Phys.* **93**, 177 (1935).

<sup>2</sup>U. Fano, *Nuovo Cimento* **12**, 154 (1935).

<sup>3</sup>M. O. Krause, in *Synchrotron Radiation Research*, edited by H. Winick and S. Doniach (Plenum, New York, 1980), Chap. 5, and references therein.

<sup>4</sup>J. A. R. Samson, in *Corpuscles and Radiation in Matter I*, Vol. XXXI of *Handbüch der Physik*, edited by W. Mehlhorn (Springer, Berlin, 1982), p. 123.

<sup>5</sup>J. H. D. Eland, cited by J. Berkowitz, *Photoabsorption, Photoionization and Photoelectron Spectroscopy* (Academic, New York, 1979).

<sup>6</sup>T. A. Carlson, P. Gerard, B. P. Pullen, and F. A. Grimm, *J. Chem. Phys.* **89**, 1464 (1988).

<sup>7</sup>A. F. Starace, *Appl. Opt.* **19**, 4051 (1980), and references therein for an extensive review.

<sup>8</sup>Proceedings of the Workshop on Some Aspects of Autoionization in Atoms and Small Molecules, Argonne National Laboratory Report No. ANL-Phy-85-3, 1985 (unpublished).

<sup>9</sup>M. J. Seaton, *Proc. Phys. Soc. London* **88**, 801 (1966).

<sup>10</sup>U. Fano, *Phys. Rev. A* **2**, 353 (1970).

<sup>11</sup>K. T. Lu, *Phys. Rev. A* **4**, 579 (1971).

<sup>12</sup>J. Geiger, *Z. Phys. A* **276**, 219 (1976); **282**, 129 (1977).

<sup>13</sup>W. R. Johnson, K. T. Cheng, K.-N. Huang, and M. Le Dourneuf, *Phys. Rev. A* **22**, 989 (1980), and references therein.

<sup>14</sup>K. Yoshino, *J. Opt. Soc. Am.* **60**, 1220 (1970).

<sup>15</sup>K. Yoshino and Y. Tanaka, *J. Opt. Soc. Am.* **69**, 159 (1979).

<sup>16</sup>K. Radler and J. Berkowitz, *J. Chem. Phys.* **70**, 216 (1979).

<sup>17</sup>K. Radler and J. Berkowitz, *J. Chem. Phys.* **70**, 221 (1979).

<sup>18</sup>P. H. Metzger and G. R. Cook, *J. Opt. Soc. Am.* **55**, 516

(1965).

<sup>19</sup>R. E. Huffman, Y. Tanaka, and J. C. Larrabee, *Appl. Opt.* **15**, 947 (1963).

<sup>20</sup>Po Lee and G. L. Weisler, *Phys. Rev.* **99**, 540 (1955).

<sup>21</sup>C. E. Moore, *Atomic Energy Levels*, Natl. Bur. Stand. (U.S.) Circ. No. 467 (U.S. GPO, Washington, D.C., 1971), Vol. III, pp. 113–117.

<sup>22</sup>R. E. Huffman, Y. Tanaka, and J. C. Larrabee, *J. Chem. Phys.* **39**, 902 (1963).

<sup>23</sup>F. M. Matsunaga, K. Watanabe, and R. S. Jackson, *J. Quant. Spectrosc. Radiat. Transfer* **5**, 329 (1965).

<sup>24</sup>K. Ueda, K. Maeda, K. Ito, and T. Namioka, *J. Phys. B* **22**, L481 (1989).

<sup>25</sup>J. A. R. Samson and J. L. Gardner, *Phys. Rev. Lett.* **31**, 1327 (1973).

<sup>26</sup>Y. Morioka, M. Watanabe, T. Akahori, A. Yasishita, and M. Nakamura, *J. Phys. B* **18**, 71 (1985).

<sup>27</sup>U. Heinzmann, F. Schäfers, K. Thimm, A. Wolcke, and J. Kessler, *J. Phys. B* **12**, L679 (1979).

<sup>28</sup>R. G. Tonkyn and M. C. White, *Rev. Sci. Instrum.* **60**, 1245 (1989).

<sup>29</sup>D. Dill, *Phys. Rev. A* **7**, 1976 (1973).

<sup>30</sup>M. O. Krause, T. A. Carlson, and P. R. Woodruff, *Phys. Rev. A* **24**, 1374 (1981).

<sup>31</sup>M. O. Krause, T. A. Carlson, and A. Fahlman, *Phys. Rev. A* **30**, 1316 (1984).

<sup>32</sup>C. D. Caldwell and M. O. Krause, *J. Phys. B* (to be published).

<sup>33</sup>B. W. Shore, *J. Opt. Soc. Am.* **57**, 881 (1967); *Rev. Mod. Phys.* **39**, 439 (1967); *Phys. Rev.* **171**, 43 (1968).

<sup>34</sup>Kiyoshi Ueda, *Phys. Rev. A* **35**, 2484 (1987).